Parametric modeling of producer gas-combustor and heat exchanger integration for micro-gas turbine application

发生气参数化建模 – 用于微型燃气轮机之燃烧器与热交换器集成

Mackay A.E. Okure[1], Wilson B. Musinguzi[2*], Terese Løvås[3]

[1]*School of Engineering, Makerere University, P.O. Box 7062, Kampala, Uganda*
[2]*Faculty of Engineering, Busitema University, P.O. Box 236, Tororo, Uganda*
[3]*Department of Energy and Process Engineering, NTNU, Trondheim, Norway*

[*]*Corresponding Author: wilson.musinguzi@gmail.com*

Abstract - **An alternative way of improving the use of biomass resources in rural areas of developing countries is to design suitable combined heat, and power (CHP) small-scale plants for distributed generation. A gasification-based CHP system can potentially have higher electricity efficiency than a direct combustion-based CHP system. The combustible gas from wood gasification is fired in a combustor that is integrated with a heat exchanger to facilitate effective heat transfer from the hot flue gases to the 100kW$_e$ micro gas turbine working fluid. Burning a gas in the combustor has an edge over the solid biomass because the gaseous fuel offers high heat exchanger temperature as well as stable combustion/continuous operation. Two parameters that have potential for efficiency advancement are investigated in this work: increased turbine inlet temperature and heat exchanger effectiveness. This paper presents a parametric model analysis of the combustion process in the combustor and heat transfer to the turbine working medium across the heat exchanger. Aspen Plus Process Modeling software (aspenONE® Engineering for Universities V7.3) was used for implementation and performing sensitivity analysis of the system. The heat exchanger and combustor integration process analysis has also shown good performance with the flue gases from combustion of producer gas providing sufficient thermal energy needed to raise the turbine working fluid to the required turbine inlet temperature. The analysis of the heat exchanger has provided parameters essential for decision making on the sizing of the heat exchanger. The practical value added was revealing the parameters needed in the design specification of the heat exchanger suitable for the heat duty of a typical 100kW$_e$ externally fired micro gas turbine based on gasification of biomass and subsequent producer gas combustion. The heat exchanger effectiveness of 0.635 was achieved in this parametric study. Furthermore, the results revealed that the heat exchanger effectiveness increased with decrease in adiabatic flame temperature. The heat duty of the hot combustion gases plays a role in the value of the adiabatic flame temperature that can give a desired effectiveness and at the same time satisfy the heat balance between the two streams.**

Keywords - **Parametric modeling, Producergas-Combustor, Heat Exchanger, Indirectly Fired Micro-gas Turbine.**

I. INTRODUCTION

An alternative way of improving the use of biomass resources in rural areas of developing countries is to design suitable combined heat and power (CHP) small-scale plants for distributed generation. Among solid biomass thermochemical conversion processes, combustion is the most advanced and market-proven one, while pyrolysis and gasification can still be considered to be at a pre-commercial stage of development according to Maraver et al. [1]. A gasification-based CHP system can potentially have higher electricity efficiency than a direct combustion-based CHP system as demonstrated in [2]-[4]. Another of its advantages is that gas firing produces less CO_2 per unit power than does a liquid or solid fuel as shown by Pilavachi [5]. According to Leilei et al. [2], small-scale biomass-fuelled CHP systems have a particularly strong relevance in improving the quality of life, especially in rural communities in developing countries. The first step in designing a CHP plant is to determine the best configuration in terms of the thermodynamic integration of all the subsystems and the

optimization of the overall energy efficiency. Bassily [6] reports the main methods for improving the efficiency or power of the combined cycle as: increasing the turbine inlet temperature (TIT), inlet air-cooling, applying gas reheat, steam or water injection into the gas turbine (GT), and reducing the irreversibility of the heat recovery steam generator (HRSG).

By replacing the combustion chamber of a gas turbine with a high temperature heat exchanger, the electrical efficiency of a solid biomass fuelled power plant can be increased from 15-20% to 25-30% [7] for typical plant sizes of 100 kWel. The main reasons why hot air gas turbines (HGT) have not succeeded until now are the high operating air temperature of over 850ºC, ash sintering, slagging and fouling, material problems on the heat exchanger due to the low heat transfer of

flue gas to air and large heat exchanger areas required as reported by Gaderer et al. [8]. In most applications, heat exchangers are very important to the overall efficiency, cost, and size of the system. Current heat exchanger designs rely heavily on fin-and-tube or plate heat exchanger designs, often constructed using copper and aluminum. Recent developments in material science, including advances in ceramics and ceramic matrix composites, open opportunities for new heat exchanger designs; Sommers et al. [9]. The major factors affecting heat exchanger performance are effectiveness, pressure drop and leakage of the heat transfer medium.

For process intensification, steam injection into the turbine working medium has shown greater increase in efficiency of externally fired microturbines due to increased specific heat of the turbine working medium. Delattin et al. [10] reports that steam addition of up to the surge limit of 3.3% of the mass of air flowing into the microturbine can increase the electric efficiency by 5%.

This paper reports on the parametric modeling of the high temperature heat exchanger and combustor integration utilizing a combustible gas from a wood gasifier for improved heat transfer to the turbine working medium. Thus the heat exchanger effectiveness is a key parameter to analyze.

II. MATERIALS AND METHODS

The researchers modeled the heat exchanger and combustor integration and analyzed its performance theoretically. The authors have carried out parametric modeling of the system to reveal the relationship of different parameters in the system in order to achieve the desired output of heat transferred to the turbine working fluid. The turbine inlet parameters are specified by the design model chosen and thus the turbine inlet temperature is set at 950ºC. Attempt to have the highest possible practical value of the key parameter of heat exchanger effectiveness and thus high heat transfer to the turbine medium was made in the analysis.

Fig. 1 illustrates the system modeled in this paper. The hot wood gas from the gasifier and preheated combustion air enter the combustor integrated with the heat exchanger. The high temperature combustion gases flow through the shell-side of

the chamber packed with heat exchanger tubes carrying the turbine working medium (air plus a small amount of steam). The heated tube-side stream is led to the gas turbine for power generation. The exhaust from the turbine is led to the heat recovery steam generator (HRSG) which delivers the steam needed for injection into compressed air at the right compressor outlet pressure. The mixing takes place at common pressure. The exhaust from combustion is used for combustion air preheating.

Thermodynamic chemical equilibrium analysis of the combustor was carried out using the RGibbs reactor. This type of reactor uses the method of direct minimization of Gibbs free energy. It is useful when the reaction stoichiometry is not known or is high in number due to many components participating in the reaction. This is the only Aspen Plus block that deals with solid, liquid and gas phase equilibrium. For the heat exchanger, the HEATX block was used for shell-and tube analysis of the flow. Both the equation of state and ideal property methods were used in the simulation to compute the thermodynamic and flow properties of the streams. The producer fuel properties in Table I published by the authors in earlier work, were used for the modeling [11], [12].

Process optimization, under atmospheric combustion and heat exchange, used thermodynamic equilibrium and exergy analysis. Aspen Plus Process Modeling software (aspenONE® Engineering for Universities V7.3) was used for implementation and performing sensitivity analysis of the system. The thermodynamic analysis of this system considers continuous deterministic steady-state conditions. Stepwise procedure with simulation using

ASPEN PLUS process modeling is used in the thermodynamic analysis of the cycle. The ASPEN PLUS Gibbs reactor was used for combustion with the assumption that the reaction follows the Gibbs equilibrium. The process parameters in the analysis were correlated with those available in the literature by Schuster et al. [13], Kentaro et al. [14], Chiaramonti et al. [15], Kautz et al. [7], Daniele et al. [16], Lieuwen et al. [17]. These parameters represent commercially available technologies or processes in advanced development stage.

Table I, Characteristic properties of the Producer gas generated in a downdraft fixed bed gasifier [11], [12].

Property	Value
Wood feed rate	0.02 (kg/s)
Steam (gasifying medium) flow rate at 500°C, 1 bar	0.012 (kg/s)
Reactor temperature in the gasification zone	820 (°C)
Net producer gas flow from the gasifier	0.028 (Nm^3/s)
Component distribution in the wood gas	43.27% H_2, 14.42% CO, 7.84% CH_4, 17.31% CO_2, 17.16% H_2O (mol(%)/mol of wood gas)
HHV of gaseous fuel	13.9 (MJ/kg)
LHV of gaseous fuel	13.4 (MJ/kG)
$\dot{m}_{pg}$	0.02 (kg/s)
Sintering temperature of the carry-over ash in wood gas	1334 (°C)

Nomenclature

Abbreviation

CHP	combined heat and power	Pr	prandtl number
HGT	hot air gas turbine	A	Cross-section area of tube (m^2)
TIT	turbine inlet temperature	D	diameter of tube (m)
ε-NTU	effectiveness number of transfer units	T	temperature (k)
Fg	flue gas	St	stanton number
GTm	gas turbine medium	UA	overall thermal conductance (kW/K)
HHV	higher heating value (MJ/kg)	Wo	wobble number
HRSG	heat recovery steam generator	$\bar{x}$	Mole fraction
LHV	lower heating value (MJ/kg)	H	Enthalpy (kJ)
LMTD	logarithmic mean temperature difference	*Greek letters*	
N	number of tubes in the heat exchanger	Δ	difference (-)
Pg	producer gas	ε	heat exchanger effectiveness
SG	specific gravity	Φ	equivalent ratio
TO	theoretical oxidant	ρ	density (kg/m^3)
GT	gas turbine	$\dot{v}$	volume flow rate (m^3/s)
		μ	dynamic viscosity (Ns/m^2)

Roman letters

n	number of moles	*Subscripts*	
C	Capacity rate (kW/K)	ad	adiabatic
h	Heat transfer coefficient (kW/m^{2}K)	i	ith component
$\bar{h}$	Enthalpy (kJ/kgmole)	o	outer
		s	surface
$\bar{h}_f^o$	Standard heat of formation (kJ/kgmole)	e	electric
$\dot{m}$	Mass flow rate, kg/s		
P	Pressure (N/m^2)		

Fig. 1, Schematic of the system under study.

III. DERIVATION OF THE PARAMETRIC MODEL OF THE COMBUSTOR AND HEAT EXCHANGER

A number of important practical issues must be addressed in designing a wood gas combustion system in order to achieve sufficient stability in the operation of the combustor/heat exchanger combination. Indeed complex interactions between combustion phenomena and fluid mechanics have been sighted as not well understood [17]. In particular, burners involve complex, less understood interactions between swirling flow dynamics, flow field alterations induced by volumetric expansion across the flame, and flame propagation.

Unlike in natural gas combustion where premixed burners are used, combustion of wood gas from the gasifier favorably utilizes non-premixed burners as portrayed by the majority of the fundamental investigations on wood gas (syngas) combustion characteristics [17]. The non-premixed burners preferred in wood gas combustion are believed to significantly lower the operability issues that are detrimental to safe combustion. This study therefore exams two important parameters namely adiabatic flame temperature and heat exchanger effectiveness as theoretical basis for the interaction between the combustor and heat exchanger system.

3.1 Adiabatic Flame Temperature

For purposes of analysis, it is assumed that the combustor operates at steady-state, steady flow conditions and that in this case, no work or power transfer occurs in addition to negligible changes in kinetic and potential energy fluxes. Energy transfer from the generated gases as heat to the surroundings (heat exchanger surfaces) due to combustion can be partly influenced by the properties of fuel burned, equivalent ratio, state of reactants (fuel and oxidant phase/temperature) and product state (completeness of combustion and product temperature) [18]. The adiabatic flame temperature gives insights on the maximum possible temperature in the combustor zone so that proper materials for combustor surfaces can be chosen for a given combustion

Flue gas Exhaust

Combustion Chamber

Heat Exchanger

Hot flue gases

Hot producer gas from gasifier

Preheated combustion air

Turbine exhaust to HRSG

Steam-air mixture

Stream Mixer

Steam from HRSG

Ambient air

Turbine

Compressor
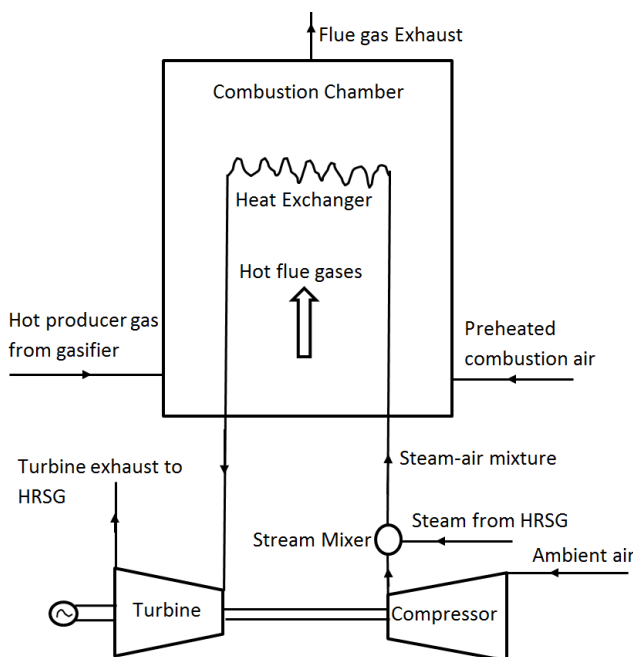
situation, and propose the necessary quenching or combustion mixture dilution (decreasing the equivalent ratio) among other interventions.

Knowing the composition of the combustible gas and taking air as the oxidant, the adiabatic temperature can be evaluated by setting a value of the equivalent ratio. Assuming one mole of wood gas, Eq. (1) then gives overall combustion expression.

$$
\left(\bar{x}_{H_2} H_2 + \bar{x}_{CO} CO + \bar{x}_{CH_4} CH_4 + \bar{x}_{CO_2} CO_2 + \bar{x}_{H_2O} H_2O \right)_{fuel}
$$
$$
+ n_{air} \frac{1}{\Phi} \left(O_2 + 3.76 N_2 \right)_{oxidant} \rightarrow \tag{1}
$$
$$
+ \left(n_{CO_2} CO_2 + n_{H_2O} H_2O + n_{air} \left(\frac{1-\Phi}{\Phi} \right) O_2 + n_{air} \frac{3.76}{\Phi} N_2 \right)_{product}
$$
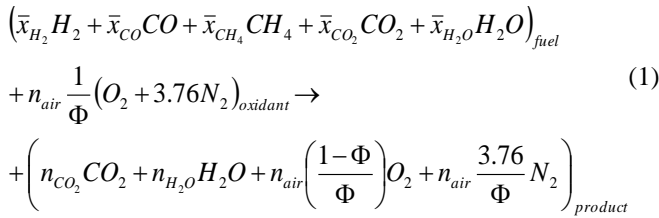
n_{CO_2}, n_{H_2O} and n_{air} are the moles of carbondioxide, water vapour and air respectively.

Substituting the known values for moles of the producer gas components from Table I and setting the value of Φ initially at 0.83333 or TO of 120, where $TO = \left(\frac{1}{\Phi} \right) 100$, Eq. (2) then balanced overall equation:

$$
0.4327 H_2 + 0.1442 CO + 0.0784 CH_4 + 0.1731 CO_2 + 0.1716 H_2O + \frac{0.44525}{\Phi} \left(O_2 + 3.76 N_2 \right) \rightarrow
$$
$$
0.3957 CO_2 + 0.7611 H_2O + 0.44525 \left(\frac{(1-\Phi)}{\Phi} \right) O_2 + (0.44525)(3.76) \left(\frac{1}{\Phi} \right) N_2
$$

$$\tag{2}$$

Performing an energy balance in the combustor at constant pressure; $H_{products} - H_{reactants} = 0$, from Eq. (2),

$$
0.4327 \left[\bar{h}_f^0 \right]_{H_2} + 0.1442 \left[\bar{h}_f^0 \right]_{CO} + 0.0784 \left[\bar{h}_f^0 \right]_{CH_4} + 0.1731 \left[\bar{h}_f^0 \right]_{CO_2}
$$
$$
+ 0.1716 \left[\bar{h}_f^0 \right]_{H_2O} + \frac{0.44525}{\Phi} \left[\left(\bar{h}_f^0 \right)_{O_2} + 3.76 \left(\bar{h}_f^0 \right)_{N_2} \right] = \tag{3}
$$
$$
0.3957 \left[\bar{h}_f^0 + \Delta \bar{h} \right]_{CO_2} + 0.7611 \left[\bar{h}_f^0 + \Delta \bar{h} \right]_{H_2O}
$$
$$
+ 0.44525 \left(\frac{1-\Phi}{\Phi} \right) \left[\bar{h}_f^0 + \Delta \bar{h} \right]_{O_2} + 0.44525(3.76) \left(\frac{1}{\Phi} \right) \left[\bar{h}_f^0 + \Delta \bar{h} \right]_{N_2}
$$

The values of $\Delta \bar{h}$ can be evaluated from appropriate tables by assuming an initial average temperature of reactant mixture in the reactor just before combustion to be around 700K since the fuel and oxidant are considered hot and preheated before the entry point, and then using trial-and-error for the unknown value of the adiabatic temperature. Standard values of enthalpy change and heat of formation are obtained from Keating [18]. The two temperature values that give the closest negative and positive value outcome in Eq. (3) are then iterated to obtain the temperature that gives zero value outcome of Eq. (3), which is taken as the estimated adiabatic flame temperature. The adiabatic temperature is evaluated for predicted equivalent ratio (Φ =1, 0.8333, 0.5, 0.4, 0.25 and 0.2) all aimed at obtaining the adiabatic temperature that is logical to minimize the temperature at which thermal NOx is likely to occur. Another important condition crucial in

combustion phenomenon is the ignition temperature; the minimum temperature at which any fuel-air mixture begins to burn. The equivalent ratio therefore has to be appropriately selected because either too much fuel above the stoichiometric amount or too much air can extinguish the flame.

3.2 Parametric Analysis of the Heat Exchanger

The objective in heat exchanger design is to enhance the thermal contact between the heat-exchanging entities, that is, to minimize the temperature difference between the heat exchanging streams and thus reducing the rate of entropy generation (exergy destruction). Hence, a heat exchanger is a multifaceted engineering system whose design involves not only the calculation of the heat transfer rate across the heat exchanger surface but also the pumping power needed to circulate the fluids, the flow arrangements, the construction of the actual hardware and the ability to disassemble the apparatus for periodic cleaning [19]. In this paper, the discussion is centered on thermal design and optimization of the heat exchanger.

The two methods commonly used for heat exchanger design and analysis are the Logarithmic Mean Temperature Difference (LMTD) and the Effectiveness Number of Transfer Units (ε-Ntu). The two methods give similar outcome for a given heat exchanger analysis problem. In the determination of heat exchanger parameters in this paper, the ε-Ntu (NTU) method is applied. A base-case for a shell-and-tube heat exchanger is considered in establishing the characteristics for the heat exchange between the combustion gases (flue gas) and the turbine working medium (air and a small amount of steam). Fig. 2 illustrates the flow arrangement for heat exchange with known parameters indicated. The microturbine parameters indicated on Fig. 2 are for a commercially available unit that is required to deliver a net power of 100 kWe. The microturbine working medium is air with steam injection (5% of flow). Parameters of the hot stream (flue gas) are obtained from the preceding discussion (sec 3.1) and the heat duty requirements in the heat exchanger.
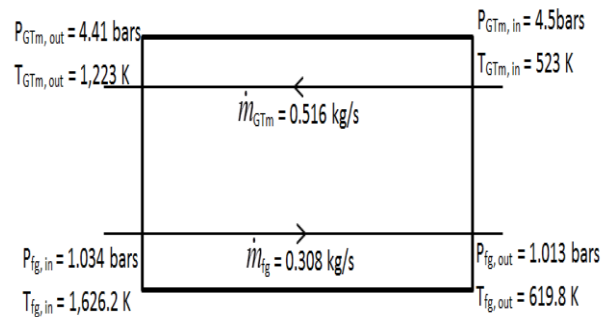
Fig. 2, Flow streams across the heat exchanger.

Compressed air and steam mixture which form the turbine working medium flows through n parallel tubes with inner diameter D, outer diameter D_o, and length L. The tubes are

mounted in a shell of cross-section area A_s. Combustion products (flue gas) flow through the tube-to-tube spaces, parallel to the tube in a counter flow mode. The problem at hand is therefore of sizing the heat exchanger i.e. determining the number of tubes and the heat exchanger dimensions. Although tubes are commercially available at only certain standard diameters and wall thicknesses, the ration $D_o/D = 1.2$ holds true in most heat exchanger tubes. To determine the remaining four unknowns; n, D, L and A_s, the analysis must satisfy the heat transfer and fluid flow relations, making use of the specified inlet and outlet temperature and pressure values across the heat exchanger.

3.2.1 Heat Transfer Relations

The capacity rate on the high pressure side (the tube side) of the heat exchanger is

$$C_{GTm} = \dot{m}_{GT}\, c_{p,GTm} = (0.516 kg/s)(1.17 kJ/kgK) = 0.6 kW/K \quad (4)$$

The capacity rate on the low pressure side can be deduced from an energy balance across the heat exchanger

$$C_{fg} = \frac{C_{GTm}(T_{GTm,out} - T_{GTm,in})}{(T_{fg,in} - T_{fg,out})} = (0.6)\frac{1,223 - 523}{1,6262 - 6198} = 0.417 kW/K \quad (5)$$

From Eq. (4) and Eq. (5), it is seen that the flow is unbalanced

$$\frac{C_{min}}{C_{max}} = \frac{C_{fg}}{C_{GTm}} \quad (6)$$

The effectiveness of the heat exchanger is obtained from

$$\varepsilon = \frac{T_{GTm,out} - T_{GTm,in}}{T_{fg,in} - T_{GTm,in}} \quad (7)$$

Then the Number of Tansfer Units is calculated as

$$NTU = \frac{\ln\left[\frac{1 - \varepsilon C_{min}/C_{max}}{1 - \varepsilon}\right]}{1 - C_{min}/C_{max}} \quad (8)$$

The overall thermal conductance is

$$UA = C\,min\,NTU \quad (9)$$

This value is related to the thermal conductances on the two sides of the heat transfer surface by

$$\frac{1}{UA} = \frac{1}{hn\pi DL} + \frac{1}{h_o n\pi D_o L} \quad (10)$$

where h and h_o are gas turbine medium-side and flue gas-side heat transfer coefficients.

3.2.2 Pressure Drop Relations

The pressure drop on the air/steam mixture stream (gas turbine working medium) is estimated from

$$\Delta P_{GTm} = f\frac{2L}{D}\frac{G^2}{\rho_{GTm}} + G^2\left(\frac{1}{\rho_{out}} - \frac{1}{\rho_{in}}\right)_{GTm} \quad (11)$$

where f is fanning friction factor, G is the mass velocity of the stream and A is the channel cross-sectional area, and

$$G = \dot{m}/A = \rho_{in}V_{in} = \rho_{out}V_{out}$$

After simplification, Eq. (11) leads to

$$f\frac{2L}{D} + 2.2455 = 42,857 n^2\left(\frac{D}{1\,m}\right)^4 \quad (12)$$

where $\quad f = f(Re_D), \quad$ and $\quad Re_D = \frac{16,850.5}{nD}$ where f is fanning friction factor.

Similar steps leading to Eq. (11) and Eq. (12) are followed for the flue gas side.

The area available for the flow of the flue gas is the difference between the total area of the shell, A_s and the area occupied by n tubes:

$$A_{fg} = A_s - \frac{n\pi D_o^2}{4} \quad (13)$$

The evaluated expression for pressure drop on the flue gas side therefore becomes:

$$f_o\frac{2L}{D_h} - 1.1 = 8,606.6\left(\frac{A_{fg}}{1\,m^2}\right)^2 \quad (14)$$

The development so far has provided one heat transfer related equation (Eq. 10) and two fluid-flow related equations (Eq. 12 and Eq. 14). These can be reduced further to obtain a final set of three equations as follows:

Invoking the Colburn analogy which relates the heat transfer and the momentum transfer for fully developed turbulent flow;

$$h = c_p GSt, \qquad St = \frac{1}{2}f\,Pr^{-2/3}; \text{ since}$$

$$UA = 0.582 kW/K, \quad G_{fg} = \frac{\dot{m}}{A_{fg}}, \text{ then Eq.(10) becomes}$$

$$1 = 0.3874\frac{D}{fL} + 0.727\frac{A_{fg}}{nf_o LD} \quad (15)$$

Since Reynolds number (Re_D) on both sides is proportional, and in the range Re_D 10^4 -10^6, the friction factor varies as $Re_D^{-0.2}$, then f and f_o are also proportional resulting into simplification of Eq. (15).

$$\frac{Re_{D_h}}{Re_D} = 0.389\frac{nD}{A_{fg}}D_h = 0.413,$$

$$\frac{f_o}{f} = \left(\frac{Re_{D_h}}{Re_D}\right)^{-0.2} = 1.1935$$

$$1 = 0.3874 + 0.61\frac{A_{fg}}{nDfL}, \quad (16)$$

Eq. (14) can then be expressed as

$$8606.6\hat{A}^3 n^2\left(\frac{D}{1\,m}\right)^4 = f\frac{2L}{D} - 1.1\hat{A} \quad (17)$$

where $\hat{A}$ is the dimensionless cross-sectional area of the flue gas stream,

$$\hat{A} = \frac{A_{fg}}{nD^2} \tag{18}$$

Eliminating the group $2fL/D$ between Eq. (12) and Eq. (17)

$$n\left(\frac{D}{1\,m}\right)^2 = \left(\frac{2.2455 + 1.1\hat{A}}{42,857 - 8,606.6\hat{A}^3}\right)^{\frac{1}{2}} \tag{19}$$

Expressing Eq. (16) in terms of $\hat{A}$ yields

$$\frac{fL}{D} = 0.3874 + 0.61\hat{A} \tag{20}$$

Combining Eq. (12) and Eq. (20)

$$n\left(\frac{D}{1\,m}\right)^2 = (7.05\ x\ 10^{-5} + 2.85\hat{A}) \tag{21}$$

With equations (16) – (21), the required numerical solution can be obtained

$$\hat{A} = 6.341\ x\ 10^{-6}$$
$$nD^2 = 9.41\ x\ 10^{-3} \tag{22}$$

Substituting the values in Eq. (18),

$$A_{fg} = \hat{A}(nD^2) = 5.97\ x\ 10^{-8}\ m^2$$

From eq. (13),

$$A_s = A_{fg} + n\frac{\pi(1.2D)^2}{4} = 0.0106 m^2$$

Noting that the shell area and the flue gas cross-section are fixed, the remaining design parameters (n, D, L) can vary, but only one can be chosen independently and must satisfy Eq. (20), i.e. $\left[\frac{fL}{D} = 0.3874\right]$ and Eq. (22). When Re_D falls in the range $10^4 - 10^6$, $f = 0.046\,Re_D^{-0.2}$ [13].

IV. RESULTS AND DISCUSSION

Table II gives the results for the values of adiabatic flame temperature at selected equivalent ratio, with resulting flow rate of the flue gas stream. The value of adiabatic flame temperature is seen to decrease with equivalent ratio. The mass flow rate of the combustion products increases as the adiabatic temperature decreases. The increase in flue gas flow is due to increase in oxidant (air) flow that result into dilution of the combustion mixture leading to decreased temperatures in the combustion zone. However the dilution which is desired for minimizing thermal stresses of the combustor materials has a limit below which it can compromise the heat duty of the flue gases for minimum permissible temperature difference in the heat exchanger flow streams. For purposes of heat exchanger analysis, the adiabatic temperature of 1626.2 K corresponding to the equivalent ratio of 0.25 is utilized as the fluegas

temperature at the heat exchanger inlet. The heat exchanger effectiveness of 0.635 was achieved for this optimization problem. For optimization purposes in the heat exchanger, it is necessary to determine the values of hot gas flow rate alongside the adiabatic flame temperature since the heat transfer to the cold fluid is dependent on both.

Table III shows the numerical results obtained by treating D as the independent variable. The values show that the variation of total heat transfer area $A = n\pi D_o L$ and overall heat transfer coefficient U with D or n is of a lesser extent. However the flow length L increases linearly with the tube diameter D. The volume of the heat exchanger $(A_s L)$ increases too due to a fixed total area of the heat exchanger. The weight of the heat exchanger is controlled by the weight of the tubes, i.e. the tube material volume $n\pi(D_0^2 - D^2)L$ increases as D increases. In conclusion, a relatively small D would be selected if a small volume or a small weight is desired for the heat exchanger, keeping in mind the associated cost requirement.

Knowing that the most important parameter for optimal performance of the heat exchanger being the increased value of the heat exchanger effectiveness, the relationship of this effectiveness with the adiabatic flame temperature is established. Fig. 3 shows the variation of the effectiveness against adiabatic flame temperature with input data given in Table 4. The effectiveness of the heat exchanger increases with decrease in adiabatic flame temperature. The heat duty of the flue gases (turbine inlet temperature) determines the lower adiabatic temperature that gives reasonably high heat exchanger effectiveness. For effectiveness outside the range $0.3 - 0.8$, the variation becomes asymptotic with reduced dependence on adiabatic temperature.

Table II, Values of adiabatic flame temperature and flue gas flow rate for given equivalent ratio Φ

Equivalent Ratio (Φ)	Adiabatic Flame Temperature (K)	Rate of flue gas flow into Heat Exchanger (kg/s)
1	2759	0.092
0.8333	2671	0.106
0.5	2101	0.164
0.4	1926	0.2
0.25	1626	0.308
0.2	1513	0.38

Table III, Heat exchanger parametric design values

D (m)	n	L (m)	Re_D 10^5	L/D	A (m^2)	U (W/m².K)
0.01	94	0.84	1	84	2.98	195
0.02	24	1.93	2	97	3.49	167
0.03	10	3.33	4	111	3.76	155
0.04	6	5.11	8	128	4.62	126

Table IV, Heat exchanger effectiveness at evaluated values of adiabatic flame temperature

Adiabatic Flame Temperature (K)	Heat exchanger effectiveness
2759	0.313
2671	0.326
2101	0.444
1926	0.500
1626	0.635
1513	0.71
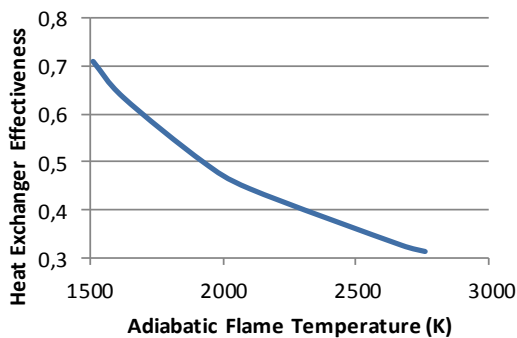
Fig. 3, Variation of heat exchanger effectiveness with adiabatic flame temperature.

V. SENSITIVITY ANALYSIS

Sensitivity analysis was performed in order to conveniently generate tables and plots showing how process performance varies with changes to selected equipment specifications and operating conditions. In the combustor, the varied parameters were the amount of oxidant (lean, stoichiometric and fuel-rich mixture of reactants) supplied and temperature in the vessel which determine the equilibrium component distributions in the hot combustion gases entering the heat exchanger. Increase in heat exchanger area led to increased turbine inlet temperature, which is essential for achieving higher system efficiency.

Aspen Plus plot wizard was used to reveal the characteristic curve of the component distribution in the vessel with varying temperature for set conditions of lean, stoichiometric and fuel-rich reactant mixture as revealed in Fig. 4, Fig. 5 and Fig. 6. As shown in Fig. 4, the combustible components in the vessel are consumed in the presence of oxygen (oxidation reaction) in attaining the equilibrium. Thereafter the components distribution (concentration) remains independent of temperature until such a high temperature value that the water-gas-shift reaction and water dissociation start to occur.

At a temperature of about 1400 K, the concentration of water vapour and carbon dioxide start to decrease as the concentration of hydrogen and carbon monoxide start to increase due the shift reaction. Increase in oxygen concentration is brought about probably by dissociation of water vapour at elevated temperatures, which also further increases the hydrogen concentration thus shifting the water-gas-shift equilibrium towards conversion of carbon dioxide to carbon monoxide. A similar trend is observed for the stoichiometric conditions of reactants in Fig. 5.

For the case of fuel-rich mixture of reactants in Fig. 6, the supply of limited oxidant meant that some concentration of the combustible components remained at equilibrium. The extent to which the insufficient oxygen reacted with the combustible components in the vessel depended on the reactivity potential of the particular component with oxygen. Initially the concentration of methane and water vapour decreases as the concentration of carbon monoxide and hydrogen increases due to the steam reforming reaction. At higher temperatures the water-gas-shift reaction favours formation of more carbon monoxide and water vapour as the concentration of carbon dioxide and hydrogen decrease.
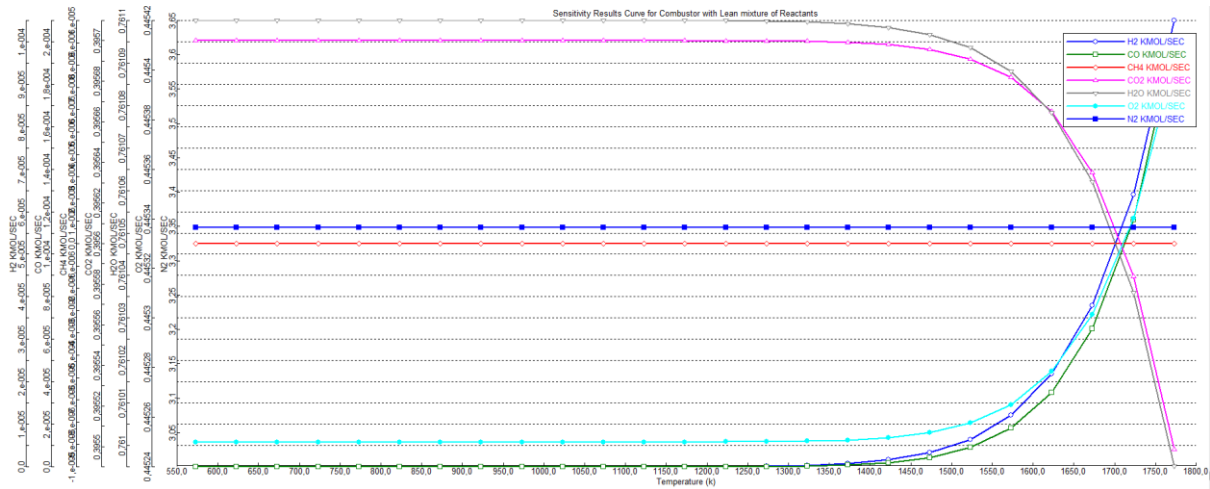
Fig. 4, Sensitivity Analysis Curve for Combustor with Lean Mixture of Reactants.
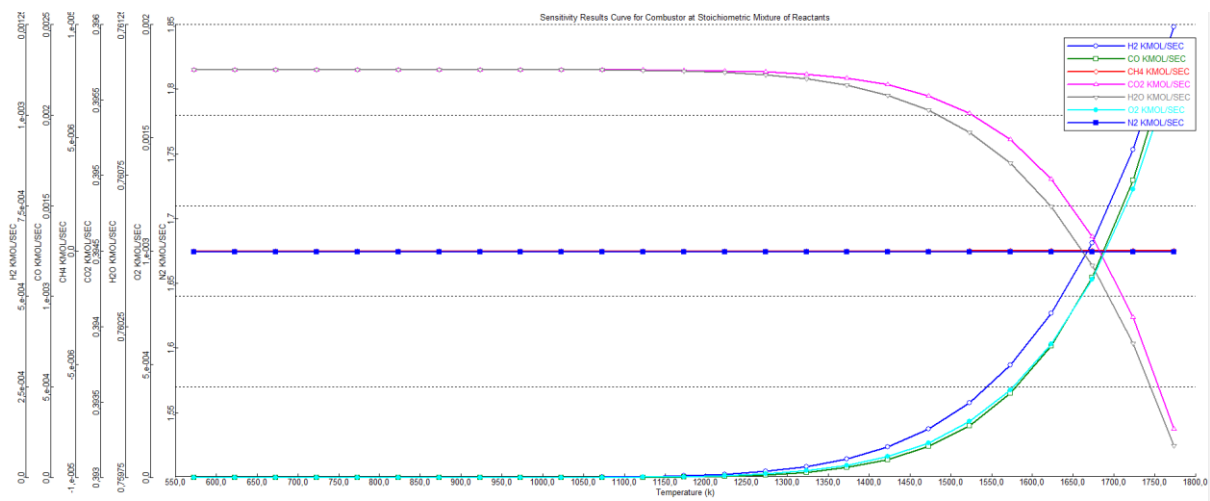
Fig. 5, Sensitivity Analysis Curve for Combustor with Stoichiometric Mixture of Reactants.
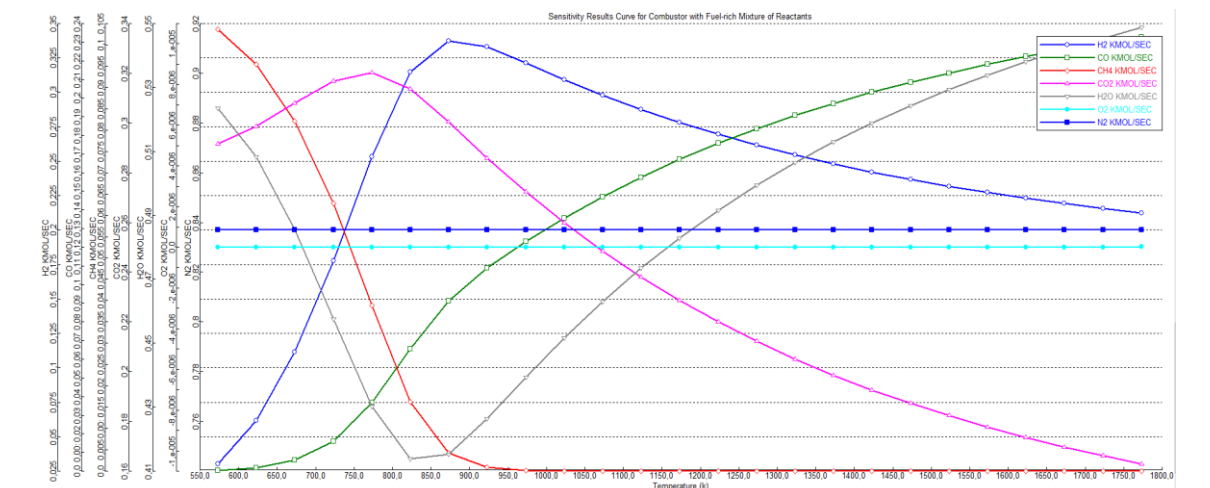
Fig. 6, Sensitivity Analysis Curve for Combustor with Fuel-rich Mixture of Reactants.

VI. CONCLUSION

The authors have carried out parametric modeling of the system to reveal the relationship of different parameters in the system in order to achieve the desired output of heat transferred to the turbine working fluid. The turbine inlet parameters are specified by the design model chosen and thus the turbine inlet temperature is set at 950°C. Though attempts to have the highest possible practical value of the key parameter of heat exchanger effectiveness and thus high heat transfer to the turbine medium were made, the author's cannot comfortably conclude that this is a generally accepted optimal value but rather a near optimal one.

The value of adiabatic flame temperature is seen to decrease with equivalent ratio. The mass flow rate of the combustion products increases as the adiabatic temperature decreases. The increase in flue gas flow is due to increase in oxidant (air) flow that results into dilution of the combustion mixture leading to decreased temperatures in the combustion zone. However the dilution which is desired for minimizing thermal stresses of the combustor materials has a limit below which it can compromise the heat duty of the flue gases for minimum permissible temperature difference in the heat exchanger flow streams. For purposes of heat exchanger analysis, the adiabatic temperature of 1626.2 K corresponding to the equivalent ratio of 0.25 is utilized as the fluegas temperature at the heat exchanger inlet. For optimization purposes in the heat exchanger, it is necessary to determine the values of hot gas flow rate alongside the adiabatic flame temperature since the heat transfer to the cold fluid is dependent on both. The stoichiometry of the combustion products determines the equilibrium concentrations and parameters of the combustion gas as revealed by the Aspen Plot wizard curves.

The analysis of combustion of the wood gas has revealed that high temperatures can be achieved in the combustor region. The heat exchanger and combustor integration process analysis has also shown good performance with the flue gases from combustion of producer gas providing sufficient thermal energy needed to raise the turbine working fluid to the required turbine inlet temperature. The analysis of the heat exchanger has provided parameters essential for decision making on the sizing of the heat exchanger. The practical value added was revealing the parameters needed in the design specification of the heat exchanger suitable for the heat duty of a typical 100kW$_e$ externally fired micro gas turbine based on gasification of biomass and subsequent producer gas combustion. The heat exchanger effectiveness of 0.635 was achieved in this parametric study. Due to high temperature involved in the process, materials that can withstand high temperature stresses have to be chosen.

The choice of a suitable Gasification system is driven by the need and local conditions at the target end user, keeping in mind that the system integration should have a good balance of being most efficient, cost effective, reliable, least polluting, sustainable in the long run and socially beneficial. Innovative systems which take into consideration the local conditions such as biomass fuel characteristics have shown great success in other countries. Therefore issues of unpredictable fuel behavior during thermochemical conversion, unreliable operating conditions, and low overall efficiency need to be addressed through continued research to make the gasification technology more attractive.

REFERENCES

[1] D. Maraver, A. Sin, J. Royo, F. Sebastián. "Assessment of CCHP systems based on biomass combustion for small-scale applications through a review of the technology and analysis of energy efficiency parameters", *Applied Energy,* **102,** pp. 1303-1313, 2013.

[2] D. Leilei, L. Hao, R. Saffa. "Development of small-scale and micro-scale biomass-fuelled CHP systems – A literature review", *Applied Thermal Engineering*, **29**, pp. 2119-2126, 2008.

[3] J.H. Juan, A.A. Guadalupe, B. Antonio. "Gasification of biomass wastes in an entrained flow gasifier: Effect of the particle size and the residence time", *Fuel Processing Technology*, **91**, pp. 681-692, 2010.

[4] M. Puig-Arnavat, C.B. Joan, C. Alberto. "Review and Analysis of Biomass Gasification models", *Renewable and Sustainable Energy Reviews*,**14**, pp. 2841-2851, 2010.

[5] P.A. Pilavachi. "Power generation with gas turbine systems and combined heat and power", *Applied Thermal Engineering*, **20**, pp. 1421-1429, 2000.

[6] A.M. Bassily. "Enhancing the efficiency and power of the triple-pressure reheat combined cycle by means of gas reheat, gas recuperation, and reduction of the irreversibility in the heat recovery steam generator", *Applied Energy*, **85**, pp. 1141-1162, 2008.

[7] M. Kautz, H. Ulf. "The externally-fired *gas-turbine* (EFGT-Cycle) for decentralized use of biomass", *Applied Energy* , **84**, pp. 795-805, 2007.

[8] M. Gaderer, G. Gallmetzer, H. Spliethoff. "Biomass fired hot air gas turbine with fluidized bed combustion", *Applied Thermal Engineering*, **30**, pp. 1594-1600, 2010.

[9] A. Sommers, Q. Wang, X. Han, C. T'Joen, Y. Park, A. Jacobi. "Ceramics and ceramic matrix composites for heat exchangers in advanced thermal systems—A review", *Applied Thermal Engineering*, **30**, pp. 2137-2152, 2010.

[10] F. Delattin, B. Svend, J.D. Ruyck. "Effects of steam injection on microturbine efficiency and performance", *Energy* , **33**, pp. 241-247, 2007.

[11] W.B. Musinguzi, M.A.E. Okure, L. Wang, A. Sebbit, T. Løvås. "Thermal characterization of Uganda's Acacia hockii, Combretum molle, Eucalyptus grandis and Terminalia glaucescens for gasification", *Biomass and Bioenergy,* **46**, pp. 402-408, 2012.

[12] W.B. Musinguzi, M.A.E. Okure, A. Sebbit, T. Løvås, I.P. Da Silva. "Thermodynamic Modeling of Allothermal Steam Gasification in a Downdraft Fixed-bed Gasifier", *Advanced Materials Research,* **875- 877**, pp. 1782 -1793, 2014.

[13] G. Schuster, G, Löffler, K. Weigl, H. Hofbauer. "Biomass steam gasification – an extensive parametric modeling study", *Bioresource Technology*, **77**, pp. 71-79, 2001.

[14] U. Kentaro, Y. Kouichi, N. Tomoaki, Y. Kunio. "High temperature *steam*-only *gasification* of woody biomass", *Applied Energy*, **87**, pp. 791-798, 2009.

[15] D. Chiaramonti, R. Giovanni, M. Francesco. "Preliminary design and economic analysis of a biomass fed micro-gas turbine plant for decentralized energy generation in Tuscany," Paper GT2004-53546, *The American Society of Mechanical Engineers (ASME) Turbo Expo proceedings*, Vienna, Austria, June 14-17,2004.

[16] C. Daniele, D. Paolo, C. Giorgio. "Performance evaluation of small size externally fired gas turbine (EFGT) power plants integrated with direct biomass dryers", *Energy* , **31**, pp. 1459-1471, 2005.

[17] T. Lieuwen, V. McDonell, D. Santavicca, T. Sattelmayer. "Burner Development and Operability Issues Associated with Steady Flowing Syngas Fired Combustors", *Combustion Science Technology*, **180**, pp.1169-1192, 2008.

[18] E.L. Keating. *Applied Combustion.* New York: Taylor & Francis Group, 2007.

[19] A. Bejan, G. Tsatsaronis, M. Moran. *Thermal Design and Optimization*. New York: John Wiley and Sons Inc., 1996.